Title

Radiation dose-escalation and dose-fractionation modulate the immune microenvironment, cancer stem cells and vasculature in experimental high-grade gliomas

Running title

Radiation modulates glioma immunity, stem cells and vasculature

Authors

Matteo Riva[1,2,*], Roxanne Wouters[1], David Nittner[3], Jolien Ceusters[1], Edmond Sterpin[4], Roberto Giovannoni[5], Uwe Himmelreich[6], Willy Gsell[6], Marc Van Ranst[7,#] and An Coosemans[1,8,#]

Affiliations

1. Department of Oncology, Laboratory of Tumor Immunology and Immunotherapy, KU Leuven, Leuven (Belgium)
2. Department of Neurosurgery, UcL Namur, Mont-Godinne University Hospital (Yvoir, Belgium)
3. Center for the Biology of Disease, KU Leuven Center for Human Genetics - InfraMouse, VIB, University of Leuven, Leuven (Belgium)
4. Department of Oncology, Laboratory of Experimental Radiotherapy KU Leuven, Leuven (Belgium)
5. Department of Biology, University of Pisa, Pisa (Italy)
6. Biomedical MRI, Department of Imaging and Pathology and Molecular Small Animal Imaging Center (MoSAIC), KU Leuven, Leuven (Belgium)
7. Laboratory for Clinical and Epidemiological Virology, Rega Institute for Medical Research, KU Leuven, Leuven (Belgium)
8. Department of Gynaecology and Obstetrics, Leuven Cancer Institute, UZ Leuven, Leuven (Belgium)

*. Corresponding Author

#. Shared senior Authors

Corresponding author

Matteo Riva

KU Leuven, Laboratory of Tumor Immunology and Immunotherapy

Herestraat 49, box 603

3000 Leuven (Belgium)

+393402523484

matteo.riva@kuleuven.be

Declarations

Ethics approval. All animal experiments were approved by the Animal Ethics Committee of the Katholieke Universiteit Leuven (project 089/2015) which follows the European Directive 2010/63/EU.

Availability of data and material. The datasets produced, used and/or analyzed during the current study are available from the corresponding author on reasonable request.

Competing interests. The Authors declare no conflict of interest.

Funding. This work was supported by the 2018 Helaers Research Prize for Neurosurgery granted to Dr. Matteo Riva and by the research grant 1527719N of the Fonds Wetenschappelijk Onderzoek (FWO) granted to Dr. An Coosemans.

Acknowledgement

We thank Prof. Thomas Seyfried for providing CT-2A cells, Gitte Thirion for helping with mice follow-up and flow-cytometry, Stijn Roden and Hilde Geeraerts for helping with mice irradiation.

Disclosures

The Authors declare no conflict of interest.

Abstract

Background. In the context of high-grade gliomas (HGGs), very little evidence is available concerning the optimal radiotherapy (RT) schedule to be used in radioimmunotherapy combinations. This studied was aimed at shedding new light in this field by analyzing the effects of RT dose escalation and dose fractionation on the tumor microenvironment of experimental HGGs.

Methods. Neurospheres (NS) CT-2A HGG-bearing C57BL/6 mice were treated with stereotactic RT. For dose-escalation experiments, mice received 2, 4 or 8 Gy as single administrations. For dose-fractionation experiments, mice received 4 Gy as a single fraction or multiple (1.33x3 Gy) fractions. The impact of the RT schedule on murine survival and tumor immunity was evaluated. Modifications of glioma stem cells (GSCs), tumor vasculature and tumor cell replication were also assessed.

Results. RT dose-escalation was associated with an improved immune profile, with higher $CD8^+$ T cells and $CD8^+$ T cells / regulatory T cells (Tregs) ratio ($p=0.0003$ and $p=0.0022$, respectively) and lower total tumor associated microglia/macrophages (TAMs), M2 TAMs and monocytic myeloid derived suppressor cells (mMDSCs) ($p=0.0011$, $p=0.0024$ and $p<0.0001$, respectively). The progressive increase of RT dosages prolonged survival ($p<0.0001$) and reduced tumor vasculature ($p=0.069$), tumor cell proliferation ($p<0.0001$) and the amount of GSCs ($p=0.0132$ or lower). Compared to the unfractionated regimen, RT dose-fractionation negatively affected tumor immunity by inducing higher total TAMs, M2 TAMs and mMDSCs ($p=0.0051$, $p=0.0036$ and $p=0.0436$, respectively). Fractionation also induced a shorter survival ($p=0.0078$), a higher amount of GSCs ($p=0.0015$ or lower) and a higher degree of tumor cell proliferation ($p=0.0003$).

Conclusions. This study demonstrates that RT dosage and fractionation significantly influence survival, tumor immunity and GSCs in experimental HGGs. These findings should be taken into account when aiming at designing more synergistic and effective radio-immunotherapy combinations.

Key words

High-grade glioma; radiotherapy; dose-escalation; dose-fractionation; tumor immunity; glioma stem cells

Introduction

The standard treatment for glioblastoma (GBM) patients includes surgical removal followed by fractionated radiotherapy (RT, 60Gy in 2Gy fractions) and Temozolomide (TMZ).[19, 27] However, despite such multimodal therapy, the prognosis of GBM patients remains extremely poor with a median survival of approximately 15 months.[7] In recent years, the evidence that RT is capable to start a potent anti-tumor immune reaction led to many clinical trials assessing the efficacy of radio-immunotherapy combinations for GBM.[6, 23]In most of them, the standard conventionally-fractionated RT regimen was used; however, it has to be taken into account that such RT schedule has been established long before the development of immunotherapy and it is therefore not optimized for this type of combination.[23, 25] To date, very limited evidence is available concerning what could be the optimal RT dosage and fractionation to be used in radio-immunotherapy combinations for GBM.[23]

In this study, we aimed at filling this knowledge gap by analyzing the effects of RT dose-escalation and dose-fractionation on the tumor microenvironment (TME) of experimental high-grade gliomas (HGG).

Methods

Experimental design. Mice were inoculated with murine high-grade glioma (HGG) CT-2A neurospheres (NS)-derived cells on day 0. Magnetic resonance imaging (MRI) was performed on day 11 in order to confirm tumor engraftment. For mice undergoing radiotherapy (RT), such MRI images were also used for the treatment planning. In the dose escalation study (Figure 1A), tumor-bearing mice were treated on day 12 with a single dose of 2, 4 or 8 Gy. Control mice were left untreated. Seventeen mice were included in each group: eight were used for survival, five were used for flow-cytometry and four were used for immunohistochemistry (IHC) analysis. In the dose fractionation study (Figure 1B), all treated mice received the same cumulative dose of 4 Gy. Such dose was administered either in one single fraction on day 12 or in three equal fractions (of 1.33 Gy each) on day 12, 13 and 14. Fifteen mice were included in each treatment group and were equally divided among survival, flow-cytometry and IHC analysis. Only for survival analysis, five untreated control mice were also included. In both the dose-escalation and dose-fractionation study, animals were randomly allocated in one of the treatment or control groups and the outcomes consisted in the analysis of mice survival, tumor-immune microenvironment, GSCs, tumor cell replication and tumor vasculature.

Ethics. All animal experiments were approved by the Animal Ethics Committee of the Katholieke Universiteit Leuven (project 089/2015) which follows the European Directive 2010/63/EU. The datasets produced, used and/or analyzed during the current study are available from the corresponding author on reasonable request.

Animals and brain tumor model. Adult C57BL/6 female mice (age: 12-14 weeks) were purchased from Envigo and were used for this study. Mice were housed in single-ventilated cages in a semi-specific pathogen free (SPF) animal facility at the Katholieke Universiteit (KU) of Leuven (Belgium). Animal welfare was monitored daily during the whole experiment period. The CT-2A NS model (NS/CT-2A) was

used in this study.[21] CT-2A cells were provided by Prof. Thomas Seyfried (Boston College, Boston, MA).[24] CT-2A NS were generated by culturing CT-2A cells in serum-free Dulbecco's Modified Eagle Medium / Nutrient Mixture F-12 (DMEM/F-12, Sigma-Aldrich) supplemented with epidermal growth factor (EGF, Thermofisher), fibroblast growth factor (FGF, Thermofisher) and B27 supplement (Thermofisher) as previously published by our group. [21] Fully formed NS were enzymatically dissociated (Stempro Accutase, Thermofisher) and $5x10^3$ NS-derived CT-2A cells, suspended in 4 µl of DMEM/F-12 medium, were stereotactically inoculated in the right striatum of the mice under general anesthesia (Ketamine/Xylazine, Bayer). Coordinates for stereotactic injection were 2.5 mm lateral from the midline, 0.5 mm anterior to the bregma and 2.5 mm below the dura mater. Tumor location was confirmed by MRI. After the generation of brain tumors, mice were weighed and clinical symptoms were evaluated at least three times per week. Mice were euthanized when they lost 20% of their initial weight and/or they reached grade 3-4 symptoms on a scoring system adapted from a previous publication.[17] Such scoring system included five grades: grade 0, no symptoms; grade 1, mild hemi-paresis (mouse moving slower than normally, with no circling behavior); grade 2, moderate hemi-paresis (mouse moving slower, instable gait with some oscillations or drops, no circling behavior); grade 3, hunch posture, severe hemi-paresis (constant circling behavior, frequent drops, impossibility to move) or both; grade 4, moribund mouse.

Magnetic resonance imaging MRI was performed on a 7T Biospec small animal MR system (Biospec 70/30, Bruker BioSpin, Ettlingen, Germany) operating underequipped with the Paravision 6.0 software (Bruker BioSpin). MR images were acquired with a quadrature volume radio-frequency coil for transmission and a mouse brain surface coil for detection (both, Bruker Biospin). Mice were anesthetized with isoflurane 1.5-2% (Baxter) and placed in a dedicated MRI compatible mouse bed. In order to avoid head movement during the scanning procedure, tooth and ear bars were used. Body temperature and respiration rate were continuously monitored through a rectal probe and respiration pillow (SA instruments, Stony Brooks, USA). Images were acquired via a quadrature volume coil (86mm

internal diameter, Bruker Biospin) for radiofrequency transmission and a mouse brain surface coil for the signal reception. Rapid acquisition relaxation enhancement (RARE) T2-weighted (T2w) images were obtained with the following parameters: RARE factor 8, repetition time / echo time 2843.5/35 ms, field of view 25×25 mm, matrix 256x256 pixels, slice thickness 0.5 mm with no slice gap.[21] Twenty-five axial-oriented slices were acquired covering the whole brain. Respiration rate and body temperature were monitored during MRI acquisition.

Radiotherapy. Stereotactic external beam image-guided arc RT was delivered by means of a Small Animal Radiation Research Platform (SAARP, Xstrahl Life Sciences) as previously published.[21] A whole-body cone-beam computed tomography (CBCT) was acquired directly on the SAARP, DICOM images from previous RARE T2w brain MRI were imported and the two sets of images were manually aligned and merged. with the corresponding brain MRI images previously obtained. The irradiation center was placed visually in the center of the tumor on the three orthogonal planes. Isodose lines confirmed that any visible tumor received the prescribed dose whereas most of the surrounding normal brain was spared. The treatment plan was administered via one 356° arc with a choice of a square collimator of 5x5 mm such that the entire tumor volume received the prescribed radiation dosage. An example of the treatment plan is visible in Figure S1. During the whole procedure, mice were kept under general anesthesia with Isoflurane 1.5-2% (Baxter).

Flow-cytometry. Flow-cytometry was used to evaluate the modification of the immune cell populations in the tumor microenvironment. On day 19 after the inoculation of tumor cells, tumor-bearing mice were deeply anesthetized (Pentobarbital, Lundbeck) and hearth-perfused with Phosphate-buffered saline (PBS). Brains were collected, mechanically disrupted and enzymatically digested with a mixture of Collagenase I (Thermofisher), Dispase I (Thermofisher) and DNAse I (Sigma Aldrich). Brain infiltrating immune cells were isolated by means of 25% Percoll gradient and stained for tumor-associated microglia/macrophages (TAMs), myeloid-derived suppressor cells (MDSCs) and T cells according to the

protocols previously published by our group.[21] Viable cells were selected based on Fixable Viability Dye (FVD) eFluor780 (Thermofisher) negativity. Total TAMs were identified as $CD45^{high}CD11b^{+}Ly6G^{-}F4/80^{+}$. Cells $Ly6C^{+}$ or $Ly6C^{-}$ were considered as inflammatory and resident TAMs, respectively. TAMs also positive for CD206 were considered alternatively-activated (M2) TAMs. Granulocytic and monocytic MDSCs (gMDSCs and mMDSCs) were identified as $CD11b^{+}Ly6G^{+}Ly6C^{-}$ and $CD11b^{+}Ly6C^{+}$ cells, respectively. Among total T cells ($CD45^{+}CD3^{+}$), $CD4^{+}$ and $CD8^{+}$ populations were identified. FoxP3-positive $CD4^{+}$ T cells cells were considered regulatory T cells (Tregs). The list of the antibodies used for flow-cytometry is available in Table S1. Samples were acquired on a BD FACSCanto II (BD Bioscience) and analyzed with the software FlowJo v.10 (FlowJo LLC).

Immunohistochemistry. IHC was used to evaluate glioma stem cells (GSCs), tumor vasculature and tumor cell proliferation. On day 19 after the inoculation of tumor cells, tumor-bearing mice were deeply anesthetized (Pentobarbital, Lundbeck) and hearth-perfused with PBS (VWR chemicals) followed by 4% paraformaldehyde (PFA). Brains were collected, submerged in 4% PFA for 48 hours, washed and paraffin-embedded (HistoStar™ Embedding Workstation). Sections of 4 µm thickness (Thermo Scientific Microm HM355S microtome) were mounted on Superfrost™ Plus Adhesion slides (Thermo Scientific) and stained. The following primary antibodies directed against the respective proteins were used to evaluate GSCs: anti-cluster of differentiation (CD) 133 (rabbit, 1:600, Abcam, ab19898), anti-Nestin (rabbit, 1:1000, Sigma, HPA026111) and anti-octamer-binding transcription factor (Oct) 4 (rabbit, 1:1000, Abcam, ab19857). Blood vessels were stained with anti-CD31 antibody (rat, 1:300, Dianova, SZ31) while cell proliferation was evaluated by means of anti phospho-Histone (PH) 3 (rabbit, 1:1000, Cell Signalling, 9701S) staining.

For all treatment/control groups analyzed, each IHC markers was assessed in 12 sections obtained from four different mice. IHC images were acquired with a Zeiss AxioScan Z1 using an x20 objective and the software ZEN 2 (Zeiss). The software ImageJ (http://rsb.info.nih.gov/ij) was used to assess CD31 stainings. The whole tumor mass was manually delineated on each section and the same color threshold

was applied to all samples in order to discriminate CD31-positive and CD31-negative areas. The CD31-positive tumor area was automatically calculated and results were expressed as percentage of tumor area covered by CD31-positive structures. The software QuPath was used to assess CD133, Nestin, Oct4 and PH3 stainings.[3] The whole tumor mass was manually delineated on each section and the watershed detection method was used for the automatic segmentation of single cells. Per staining, five to ten positive and five to ten negative cells were manually identified in one random sample and used to create a "cell classifier" with the relative built-in function of the software. Such classifier was then applied to all samples (of the same staining) and the number of positive and negative cells was automatically calculated. Results were expressed as percentage of positive cells over total tumor cells. The granule layer of the cerebellum, the large vessels in the subarachnoid space of the brains and the olfactory bulbs were used as positive IHC controls for GSC markers, CD31 and PH3, respectively. The semi-oval center of the contralateral healthy brain was used as negative control for all stainings.

Statistical analysis. Statistical analysis was performed using Prism v.8.0 (Graphpad Software) and a 2-tailed p-value <0.05 was considered significant. Survival data were expressed as medians and compared using log-rank (Mantel-Cox) test. Adjustment for multiple survival comparisons was performed with Benjamini-Hochberg method. In the dose-escalation experiments, flow-cytometry and IHC data underwent a primary and a secondary analysis. For the primary analysis, the radiation dose was considered as a continuous variable and the correlation between increasing RT dosages and modification of immune cells or IHC parameters was tested via Pearson's r and linear regression. For the secondary analysis, the radiation dosage was considered as a discrete variable. Data were tested for normal distribution using D'Agostino-Pearson (if $n\geq8$) or Shapiro-Wilk (if $n<8$) test. Normally distributed data were expressed as means and standard deviations, and compared using parametric ANOVA. Non-normally distributed data were expressed as medians and interquartile ranges, and compared using non-parametric Kruskal-Wallis test. In dose-fractionation experiments, the RT dosage was considered as discrete variable. As for dose-escalation experiments, data were tested for normal distribution and

expressed accordingly. Normally distributed data were then compared by using the unpaired t test with Welch's correction, non-normally distributed data were compared by using the Mann-Whitney test.

Results

Higher radiation dosages are associated with prolonged survival, more favorable immune profile and reduced GSCs, tumor vasculature and tumor cell replication

In the dose-escalation study, mice were treated with 2, 4 or 8 Gy RT administered in one single fraction. Control mice were left untreated. As depicted in Figure 2, treated mice survived significantly longer than untreated controls and the RT dose-escalation induced a progressive increase of survival (Log-rank $p<0.0001$). Median survival was 26 days for control mice, 31 days for mice receiving 2 Gy ($p_{adj}=0.0075$ versus controls) and 36 days for mice receiving 4Gy ($p_{adj}=0.0239$ versus 2Gy). The median survival was not reached for mice receiving 8 Gy, since in this group we observed 75% long-term survivors ($p_{adj}=0.005$ versus 4 Gy).

The primary and the secondary analysis consistently showed that RT dose-escalation positively modulated tumor immunity by inducing a progressive increase of anti-tumor immune cells and a progressive decrease of immune suppressive cells in the context of both the adaptive and innate system. In the primary analysis (Figure 3), increasing RT dosages were associated with an increase in $CD8^+$ T cells ($b_{RTdosage}=1.168$, $p=0.0003$) and $CD8^+$ T cells / regulatory T cells (Tregs) ratio ($b_{RTdosage}=0.292$, $p=0.0022$) whereas a decrease in total TAMs ($b_{RTdosage}=-1.847$, $p=0.0011$), immunosuppressive M2 TAMs ($b_{RTdosage}=-0.994$, $p=0.0024$) and monocytic (m) MDSCs ($b_{RTdosage}=-0.468$, $p<0.0001$) was observed. No significant association was found between the radiation dosage and $CD4^+$ T cells, Tregs and granulocytic (g) MDSCs ($p=0.1725$, $p=0.1232$ and $p=0.9844$ respectively). The secondary analysis provided similar results; however, the differences in TAMs did not reach statistical significance because of the relatively large standard deviation (Figure S2).

The IHC assessment of GSCs, tumor vasculature and tumor cell replication was performed at the same time point of the immune analysis. As shown in Figure 4, the primary analysis demonstrated the positive impact of dose escalation on GSCs since the increase of RT dosages was negatively associated with all the three GSCs markers analyzed: Nestin ($b_{RTdosage}=-0.733$, $p<0.0001$),

CD133 ($b_{RTdosage}$ -0.891, p=0.0132) and Oct4 ($b_{RTdosage}$=-1.524, p=0.0011). A significant decrease of the proportion of replicating tumor cells (PH3 staining) and a trend towards a reduction of CD31+ tumor vessels were also observed ($b_{RTdosage}$=-2.374, p<0.0001 and $b_{RTdosage}$=-0.230, p=0.0690 respectively). The results of the secondary analysis confirmed those of the primary; however, statistical significance was not reached for CD133+ GSCs due to the relatively large standard deviation (Figure S3). Representative IHC images of Nestin, CD133, Oct4, CD31 and PH3 stainings in the dose-escalation study are shown in Figure S4.

Fractionated RT is associated with shorter survival and less favorable immune profile, and it has a reduced efficacy in the context of GSCs and tumor cells replication

In the dose-fractionation study, all treated mice received the same cumulative RT dose of 4 Gy which was either given in one single administration or divided in three equal fractions of 1.33 Gy. A control group of untreated mice was included only in the survival analysis. As shown in Figure 5, RT dose-fractionation had a negative impact on mice survival. Unfractionated RT significantly prolonged survival compared to controls (36 vs 27 days, p_{adj}=0.0228). Conversely, such survival advantage was completely lost in case of fractionated RT, since mice undergoing this treatment survived significantly shorter than those undergoing the unfractionated regimen (30 vs 36 days, p_{adj}=0.0117). Furthermore, the survival of mice treated with fractionated RT was not different from that of the controls (30 vs 27 days, p_{adj}=0.31).

As shown in Figure 6, RT dose-fractionation had a negative impact on the innate immunity, inducing higher total TAMs (p=0.0051), M2 TAMs (p=0.0036) and mMDSCs (p=0.0436) compared to the unfractionated regimen. Of note, mice treated with fractionated RT exhibited significantly lower gMDSC (p=0.0450); however, this cell type was approximately ten times less abundant than its monocytic counterpart. Conversely, no significant differences in T cells populations were observed. $CD8^+$ T cells and $CD4^+$ T cells were comparable in the fractionated and unfractionated regimens (p=0.6052 and p=0.9604, respectively). We found a trend towards lower Tregs in the fractionated RT group (p=0.0639),

however the $CD8^+$ T cells / Tregs ratio, which provides an indication about the balance between immune activation and immune suppression, was comparable in the two treatment groups (p=0.6031). Unfractionated RT was also more effective in eliminating GSCs compared to the fractionated schedule (Figure 7). In particular, tumors irradiated with one single dose of 4 Gy significantly showed lower $Nestin^+$ and $Oct4^+$ GSCs compared to those irradiated with three doses of 1.33 Gy each (p=0.0015 and p=0.001 respectively). No differences were observed in the context of $CD133^+$ GSCs (p=0.189). The unfractionated regimen was more effective in reducing tumor cells proliferation (p=0.0003) while tumor vasculature was similar in the two treatment groups (p=0.6707). Representative IHC images of Nestin, CD133, Oct4, CD31 and PH3 stainings in the dose-fractionation study are shown in Figure S5.

Discussion

In recent years, many preclinical studies demonstrated that RT could potentiate the effects of cancer immunotherapy.[12, 15, 22] Therefore, a number of clinical trials evaluating the efficacy of radio-immunotherapy combinations in patients, including those diagnosed with HGG, has been started.[20] However, two important issues prevent from directly translating into HGG patients the results obtained in radio-immunotherapeutic animal studies. First, most preclinical evidence concerning the immune effects of RT in cancer has not been obtained in HGG models: this could have relevant consequences given the peculiar aspects of the brain's immune system.[8] Second, there is an important methodological difference between the available HGG preclinical studies and the ongoing clinical trials: rodents are usually treated with one single RT administration, while HGG patients are being treated (with few exceptions) with the usual conventionally-fractionated RT schedule (30 x 2 Gy).[2] Well-established evidence proves that RT can potentiate the anti-tumor immune reaction; nevertheless, it has also been shown that RT can be immune suppressive.[5, 6, 22, 23, 25, 26] In this balance between immune activation and suppression, RT dosage and fractionation play a critical role.[2, 10, 22, 25] Interestingly, this differential immune modulation might become apparent only when RT is combined with immunotherapy: in the same breast carcinoma models, two different RT regimens had equal effects when used alone but showed different efficacy in combination with checkpoint blockade.[11] All this demonstrates that the optimal RT schedule for radio-immunotherapy combinations still has to be defined, in particular for HGGs. The present study was specifically aimed at addressing this knowledge gap.[20, 23, 25]

This study was performed using the NS/CT-2A model, a fully immunocompetent orthotopic HGG model recently developed by our group.[21] When RT was administered in one single session, dose escalation was positively associated with survival and the highest RT dosage (8 Gy) was also capable to cure 75% of the animals. This can be explained by immune and non-immune phenomena. In term of immune effects, we demonstrated not only that single-fraction RT can positively modulate HGG

immunity (confirming previous literature)[20] but also that such modulation is dose dependent and involves both the adaptive and innate immune compartments. In terms of non-immune effects, we showed that RT dose escalation is negatively associated with the expression of PH3, a proliferation marker which has been reported to be potentially more accurate than Ki67[14]. In line with the traditional radio-biological concepts, this is explained by the capacity of ionizing radiations to induce DNA damage which is followed by cell-cycle arrest and apoptosis.[6] To dissect the immunological role of RT dose-fractionation, we treated NS/CT-2A tumor-bearing mice with a cumulative dosage of 4 Gy given either in one single administration or fractionated in three equal doses. Such dosage was chosen since it provided the strongest survival benefit without generating any long-term survivor: this is in line to what is observed in HGG patients where RT alone does not allow for a definitive cure.[27] Interestingly, mice receiving the single irradiation survived significantly longer than mice undergoing the fractionated regimen, which in turn had a survival comparable to controls. We did not find significant differences in term of adaptive immunity between these two RT schedules. However, significantly higher innate immune-suppressive cells (total TAMs, M2 TAMs and mMDSCs) were found following the fractionated regimen. In addition, tumors treated with single-dose RT showed a significantly lower cell replication. Taken together, our results show the positive impact of RT dose-escalation and the negative impact of RT dose-fractionation on HGG immunity.

Another area of active research concerns GSCs, a subpopulation of HGG cells which has been shown to contribute to the HGG radio-resistance due to their increased capacity of DNA repair.[1, 4, 9, 13, 16, 18] In the present study, we investigated the impact of RT dose escalation and fractionation on GSCs by evaluating the expression of three GSCs markers (Nestin, CD133 and Oct4), two of which (Nestin and CD133) have been recently proven to be associated with a significantly worse prognosis in a recent meta-analysis.[28] In our experiments, RT dose-escalation reduced the expression of all the three GSC markers analyzed. Conversely, mice receiving fractionated RT showed significantly higher amounts of $Nestin^+$ and $Oct4^+$ GSCs compared to mice receiving unfractionated RT. These results indicate that RT

dosage and fractionation influences the GSC niche in HGG. Similarly to tumor immunity, also in this case the dose-fractionation had a detrimental impact whereas the dose-escalation had a positive impact.

This study suffers some limitations. First, the experiments were performed in one single tumor model (NS/CT-2A). However, the NS/CT-2A was specifically designed to assess immune suppression, GSCs and vascular proliferation; therefore, it is particularly suitable for this type of studies.[21] Second, tumor infiltrating immune cells were analyzed only with flow-cytometry which does not provide information concerning the spatial location of such cells. However, this technique allows for a detailed characterization of several subtypes of immune cells which would have been not possible with other techniques such as IHC (for example MDSC). Third, the RT dosages used in this study do not correspond exactly to what is used in the clinic. This was due to the higher responsiveness to ionizing radiations of NS/CT-2A tumors compared to human gliomas. However, we explored a broad range of dosages from 2 Gy (which corresponds to the single fractionations given to patients in the standard fractionated regimen) until 8 Gy (which induced 75% of long term survivors, an effect much stronger than what is seen in patients). Furthermore, for the dose-fractionation experiments, we used cumulative dosages (4Gy) which was able to prolong survival without inducing long-term survivors: this closely mimics what observed in GBM patients.

Conclusions

Many clinical trials combining RT and immunotherapy for the treatment of malignant gliomas are currently ongoing. Nevertheless, very limited evidence is available concerning the optimal RT schedule to be used in such radio-immunotherapy combinations. In this study, we demonstrated for the first time that dose escalation and fractionation have a strong impact on the immune microenvironment of experimental malignant gliomas. In particular, RT dose-escalation is associated with a more favorable immune profile whereas RT dose-fractionation is immunologically detrimental. Similarly, fractionated RT shows a lower efficacy in eliminating GCSs and reducing tumor cell proliferation compared to the unfractionated treatment. These results might have relevant implications for future clinical trials, given that most HGG patients receiving radio-immunotherapy combinations are treated with a fractionated regimen.

References

1. Abou-Antoun TJ, Hale JS, Lathia JD, Dombrowski SM (2017) Brain Cancer Stem Cells in Adults and Children: Cell Biology and Therapeutic Implications. Neurotherapeutics 14(2):372–384
2. Arnold KM, Flynn NJ, Raben A, Romak L, Yu Y, Dicker AP, Mourtada F, Sims-Mourtada J The Impact of Radiation on the Tumor Microenvironment: Effect of Dose and Fractionation Schedules. Cancer Growth Metastasis 11:eCollection 2018
3. Bankhead P, Loughrey MB, Fernandez JA, et al (2017) QuPath: Open source software for digital pathology image analysis. Sci Rep 7(1):16878
4. Bao S, Wu Q, McLendon RE, Hao Y, Shi Q, Hjelmeland AB, Dewhirst MW, Bigner DD, Rich JN (2006) Glioma stem cells promote radioresistance by preferential activation of the DNA damage response. Nature 444(7120):756–760
5. Bernier J (2016) Immuno-oncology: Allying forces of radio- and immuno-therapy to enhance cancer cell killing. Crit Rev Oncol Hematol 108:97–108
6. Bernier J, Hall EJ, Giaccia A (2004) Radiation oncology: a century of achievements. Nat Rev Cancer 4(9):737–747
7. Bianco J, Bastiancich C, Jankovski A, des Rieux A, Préat V, Danhier F (2017) On glioblastoma and the search for a cure: where do we stand? Cell Mol Life Sci 74(13):2451–2466
8. Brown NF, Carter TJ, Ottaviani D, Mulholland P (2018) Harnessing the immune system in glioblastoma. Br J Cancer 119(10):1171–1181
9. Chen J, Li Y, Yu T-S, McKay RM, Burns DK, Kernie SG, Parada LF (2012) A restricted cell population propagates glioblastoma growth after chemotherapy. Nature 488(7412):522–6
10. Demaria S, Formenti SC Radiation as an immunological adjuvant: current evidence on dose and fractionation. Front Oncol 2:eCollection 2012
11. Dewan MZ, Galloway AE, Kawashima N, Dewyngaert JK, Babb JS, Formenti SC, Demaria S (2009) Fractionated but not single-dose radiotherapy induces an immune-mediated abscopal effect

when combined with anti-CTLA-4 antibody. Clin Cancer Res 1(17):5379–5388

12. Formenti SC, Demaria S (2013) Combining radiotherapy and Cancer Immunotherapy: a Paradigm Shift. 105(4):256–265

13. Hasslacher S, Schneele L, Stroh S, et al (2018) Inhibition of PI3K signalling increases the efficiency of radiotherapy in glioblastoma cells. Int J Oncol 53(5):1881–1896

14. Kim J-Y, Jeong HS, Chung T, Kim M, Lee JH, Jung WH, Koo JS (2017) The value of phosphohistone H3 as a proliferation marker for evaluating invasive breast cancers: A comparative study with Ki67. Oncotarget 8(39):65064–65076

15. Leaman Alcibar O, Candini D, Lopez-Campos F, et al (2019) Time for radioimmunotherapy: an overview to bring improvements in clinical practice. Clin Transl Oncol 21(8):992–1004

16. Liu J, Gao Q, Xie T, Liu Y, Luo L, Xu C, Shen L, Wan F, Lei T, Ye F (2018) Synergistic effect of TRAIL and irradiation in elimination of glioblastoma stem-like cells. Clin Exp Med 18(3):399–411

17. Maes W, Rosas GG, Verbinnen B, Boon L, De Vleeschouwer S, Ceuppens JL, Van Gool SW (2009) DC vaccination with anti-CD25 treatment leads to long-term immunity against experimental glioma. Neuro Oncol 11(5):529–542

18. Morokoff A, Ng W, Gogos A, Kaye AH (2015) Molecular subtypes, stem cells and heterogeneity: Implications for personalised therapy in glioma. J Clin Neurosci 22(8):1219–1226

19. Ostrom QT, Gittleman H, Fulop J, Liu M, Blanda R, Kromer C, Wolinsky Y, Kruchko C, Barnholtz-Sloan JS (2015) CBTRUS Statistical Report: Primary Brain and Central Nervous System Tumors Diagnosed in the United States in 2008-2012. Neuro Oncol 17 Suppl 4:iv1–iv62

20. Reznik E, Smith AW, Taube S, Mann J, Yondorf MZ, Parashar B, Wernicke AG (2018) Radiation and Immunotherapy in High-grade Gliomas: Where Do We Stand? Am J Clin Oncol Cancer Clin Trials 41(2):197–212

21. Riva M, Wouters R, Weerasekera A, et al (2019) CT-2A neurospheres-derived high-grade glioma in mice: a new model to address tumor stem cells and immunosuppression. Biol Open 8(9):bio044552

22. Rückert M, Deloch L, Fietkau R, Frey · Benjamin, Hecht M, Udo ·, Gaipl S (2018) Immune modulatory effects of radiotherapy as basis for well-reasoned radioimmunotherapies. Strahlenther Onkol 194(6):509–519

23. Sahebjam S, Sharabi A, Lim M, Kesarwani P, Chinnaiyan P (2017) Immunotherapy and radiation in glioblastoma. J Neurooncol 134(3):531–539

24. Seyfried TN, el-Abbadi M, Roy ML (1992) Ganglioside distribution in murine neural tumors. Mol Chem Neuropathol 17(2):147–167

25. Sharabi AB, Lim M, DeWeese TL, Drake CG (2015) Radiation and checkpoint blockade immunotherapy: radiosensitisation and potential mechanisms of synergy. Lancet Oncol 16(13):e498–e509

26. Song X, Shao Y, Jiang T, et al (2018) Radiotherapy Upregulates Programmed Death Ligand-1 through the Pathways Downstream of Epidermal Growth Factor Receptor in Glioma. EBioMedicine 28:105–113

27. Stupp R, Mason WP, Van Den Bent MJ, et al (2005) Radiotherapy plus concomitant and adjuvant temozolomide for glioblastoma. N Engl J Med 352(10):987–996

28. Wu B, Sun C, Feng F, Ge M, Xia L (2015) Do relevant markers of cancer stem cells CD133 and Nestin indicate a poor prognosis in glioma patients? A systematic review and meta-analysis. J Exp Clin Cancer Res 34(1):44

Figure legends

Figure 1. Experimental plan. In the first set of experiment (dose escalation, A), mice were treated with 2, 4 or 8 Gy delivered in one single administration. In the second set of experiments (dose fractionation, B), mice were treated with a cumulative dose of 4 Gy delivered in one single administration or fractionated in three equal doses of 1.33 Gy each. In both cases, control animals were left untreated. Experimental readouts were mice survival and the modification of the tumor microenvironment. NS: neurospheres; IHC: immunohistochemistry; MRI: magnetic resonance imaging.

Figure 2. Survival of mice following RT dose-escalation. NS/CT-2A HGG-bearing mice were treated with 2, 4 or 8 Gy given in one single administration while control mice were left untreated. All treated mice survived significantly longer (p_{adj}=0.0075, padj=0.00025 and p=0.005 for 2, 4 and 8 Gy, respectively) than control mice and the increase of the radiation dose was associated with increased survival. Survivals were compared by using the log-rank (Mantel-Cox) test and adjustment for multiple survival comparisons was performed with Benjamini-Hochberg method.

Figure 3. Modifications of the tumor-immune microenvironment induced by RT dose-escalation. NS/CT-2A HGG-bearing mice were treated with 2, 4 or 8 Gy given in one single administration while control mice were left untreated. Tumor-infiltrating immune cells were analyzed with flow-cytometry seven days after the treatment. In the adaptive immune compartment (panel A, B, C and D), the RT dose-escalation was positively correlated with $CD8^+$ T cells and the $CD8^+$ T cells / Tregs ratio. No correlation were seen between the radiation dose and $CD4^+$ T cells or Tregs. In the innate immune compartment (panel E, F, G and H), the RT dose-escalation was negatively correlated with total TAMs, M2 TAMs and mMDSCs. No correlation was found between the radiation dose and gMDSCs. Immune cells are expressed as percentage of $CD45^+$ cells. CD: cluster of differentiation; Tregs: regulatory T cells; TAMs:

tumor associated macrophages/microglia; m and gMDSCs: monocytic and granulocytic myeloid-derived suppressor cells

Figure 4. Impact of RT dose-escalation on GSCs, tumor vasculature and tumor cell replication. NS/CT-2A HGG-bearing mice were treated with 2, 4 or 8 Gy given in one single administration while control mice were left untreated. Seven days after treatment, brains were collected and stained for immunohistochemistry. RT dose-escalation was negatively correlated with the expression of the GSC markers Nestin (A), CD133 (B) and Oct4(C). The increase of the radiation dosage induced a tendency towards a reduction of the tumor vasculature (D) and was negatively correlated with the proliferation marker PH3. HGG: high-grade gliomas; CD: cluster of differentiation; Oct4: octamer-binding transcription factor 4; PH3: phosphohistone H3.

Figure 5. Survival of mice following RT dose-fractionation. NS/CT-2A HGG-bearing mice were treated with a cumulative dosage of 4 Gy, which was delivered either in one single administration or in three equal fractions of 1.33 Gy each. Control mice were left untreated. Mice treated with the unfractionated regimen survived significantly longer than mice receiving fractionated RT and controls. The survival of mice treated with the fractionated regimen did not differ from controls. Survivals were compared by using the log-rank (Mantel-Cox) test and adjustment for multiple survival comparisons was performed with Benjamini-Hochberg method.

Figure 6. Modifications of the tumor-immune microenvironment induced by RT dose-fractionation. NS/CT-2A HGG-bearing mice were treated with a cumulative dosage of 4 Gy, which were delivered either in one single administration or in three equal fractions of 1.33 Gy each. Tumor-infiltrating immune cells were analyzed with flow-cytometry seven days after the start of the treatment. No significant differences were found in the analysis of the adaptive compartment of the tumor-immune micro environment (panel A, B, C and D). Conversely, differences were seen in the innate immune system

where unfractionated RT induced a better immune profile with significantly lower total TAMs, M2 TAMs and mMDSCs (panel E, F and G, respectively). On the contrary, gMDSCs showed the opposite behavior and where significantly higher in the after unfractionated RT. Immune cells are expressed as percentage of $CD45^+$ cells. CD: cluster of differentiation; Tregs: regulatory T cells; TAMs: tumor associated macrophages/microglia; m and gMDSCs: monocytic and granulocytic myeloid-derived suppressor cells

Figure 7. Impact of RT dose-fractionation on GSCs, tumor vasculature and tumor cell replication. NS/CT-2A HGG-bearing mice were treated with a cumulative dosage of 4 Gy, which were delivered either in one single administration or in three equal fractions of 1.33 Gy each. Seven days after the start of treatment, brains were collected and stained for IHC. $Nestin^+$ (A) and $Oct4^+$ GSCs were significantly lower after the unfractionated RT compared to fractionated RT, while no significant differences were found in the expression of CD133 (C). CD: cluster of differentiation; Oct4: octamer-binding transcription factor 4; PH3: phosphohistone H3.

Authors contributions.

Conception of the study: Matteo Riva, An Coosemans, Marc van Ranst, Roberto Giovannoni

Design of the experiments: Matteo Riva, An Coosemans

Radiotherapy: Matteo Riva, Roxanne Wouters, Edmond Sterpin, Uwe Himmelreich

Flow-cytometry: Matteo Riva, Roxanne Wouters

Immunohistochemistry: Matteo Riva, Roxanne Wouters , David Nittner

Analysis and interpretation of the results: Matteo Riva, Jolien Ceusters, An Coosemans, Marc van Ranst, Roberto Giovannoni

Manuscript writing: Matteo Riva

All authors read, reviewed and approved the final version of the manuscript.

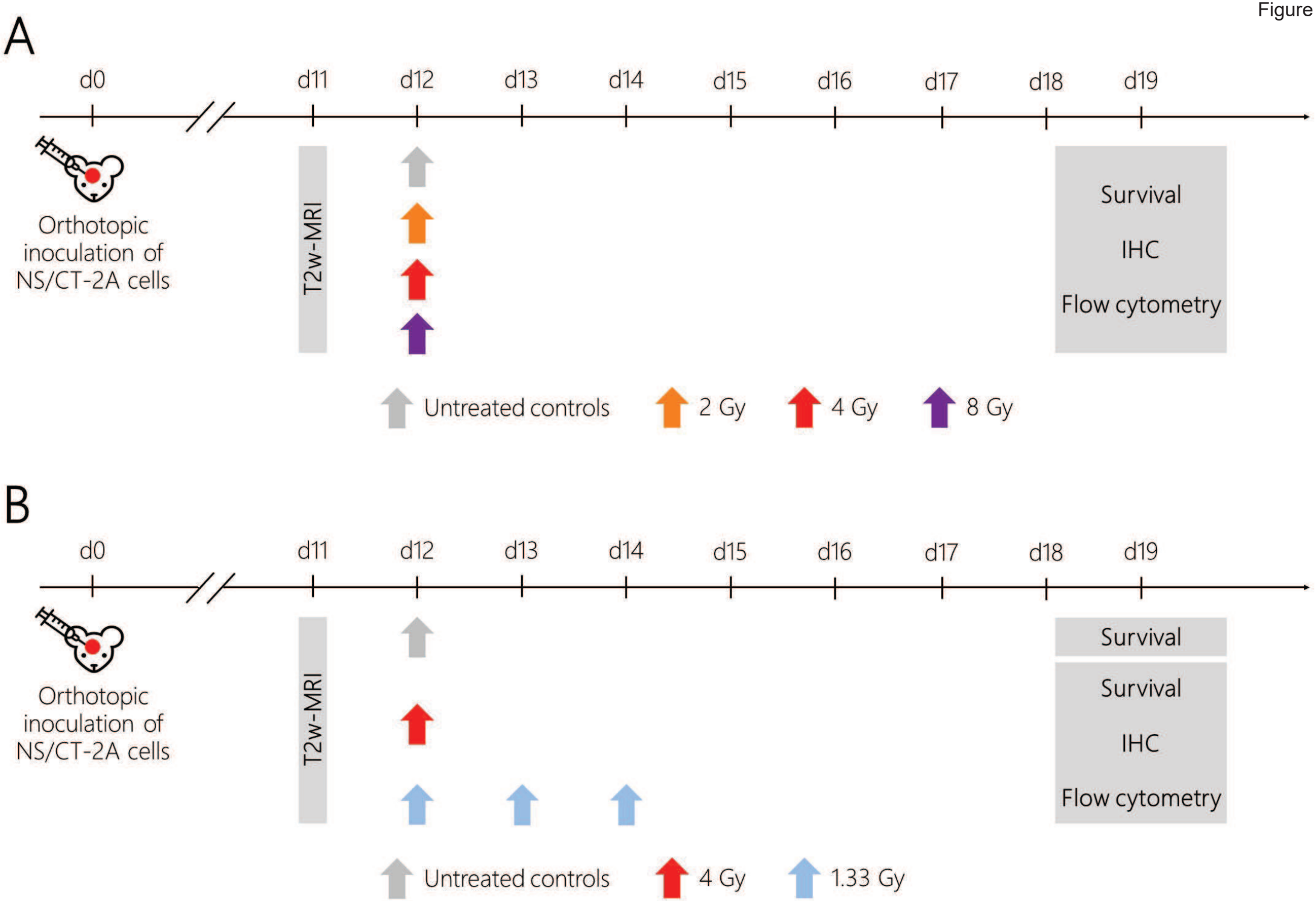
A
d0
d11
d12
d13
d14
d15
d16
d17
d18
d19
Orthotopic inoculation of NS/CT-2A cells
T2w-MRI
Survival
IHC
Flow cytometry
Untreated controls
2 Gy
4 Gy
8 Gy
B
d0
d11
d12
d13
d14
d15
d16
d17
d18
d19
Orthotopic inoculation of NS/CT-2A cells
T2w-MRI
Survival
Survival
IHC
Flow cytometry
Untreated controls
4 Gy
1.33 Gy

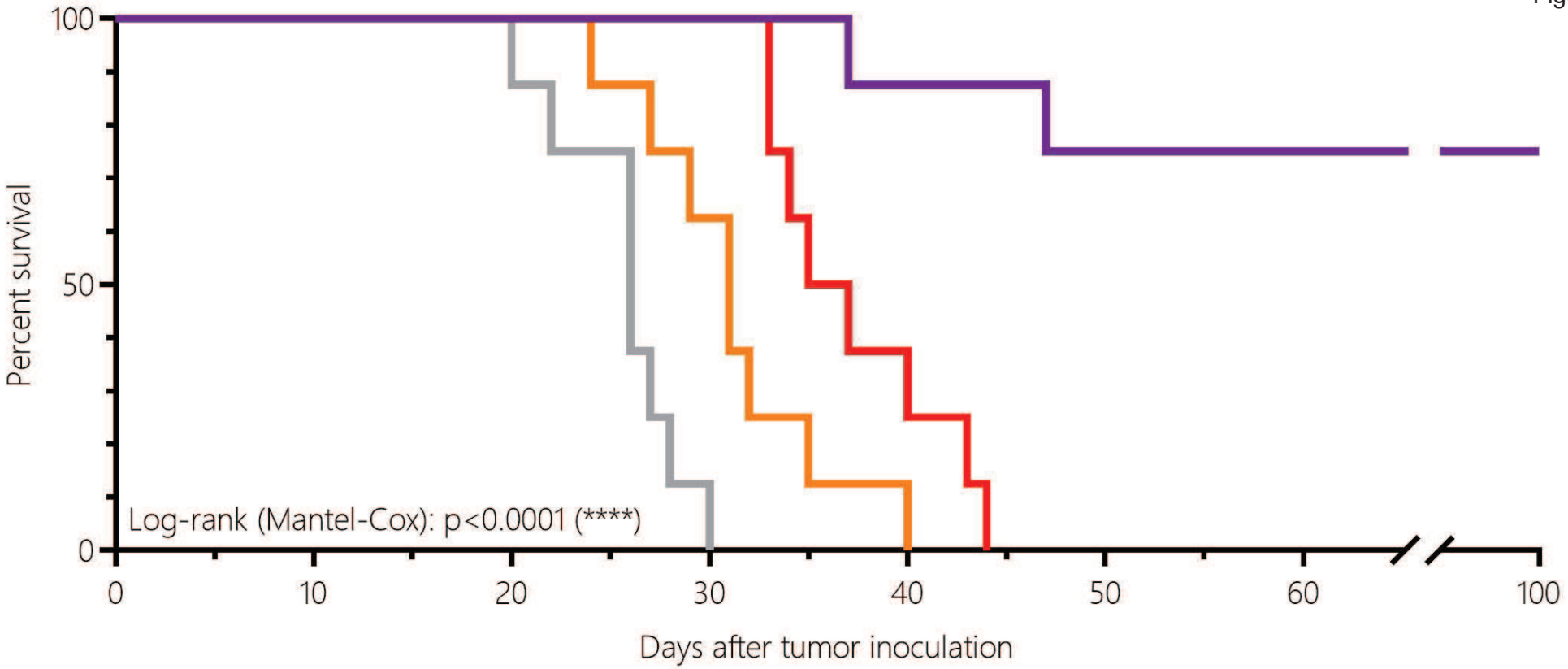

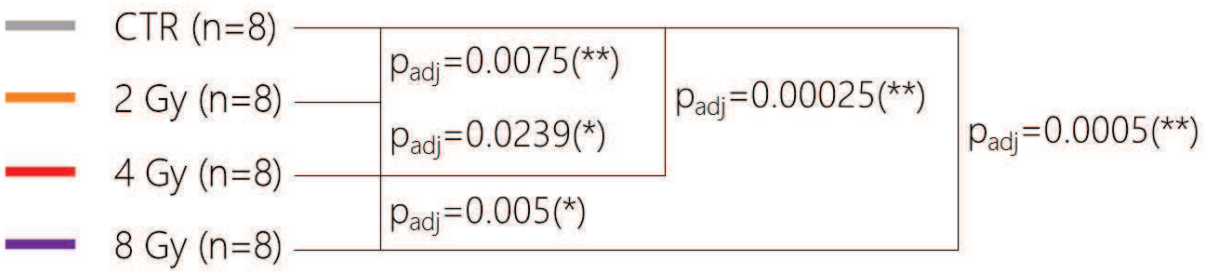

Comparison	Original P value	Benjamini-Hochberg adjusted P value	Benjamini-Hochberg P value threshold	Significant
CTR vs 4 Gy	0.0001	0.00025	0.01	Yes (**)
CTR vs 8 Gy	0.0001	0.0005	0.02	Yes (**)
4Gy vs 8Gy	0.003	0.005	0.03	Yes (*)
CTR vs 2 Gy	0.006	0.0075	0.04	Yes (**)
2Gy vs 4Gy	0.0239	0.0239	0.05	Yes (*)

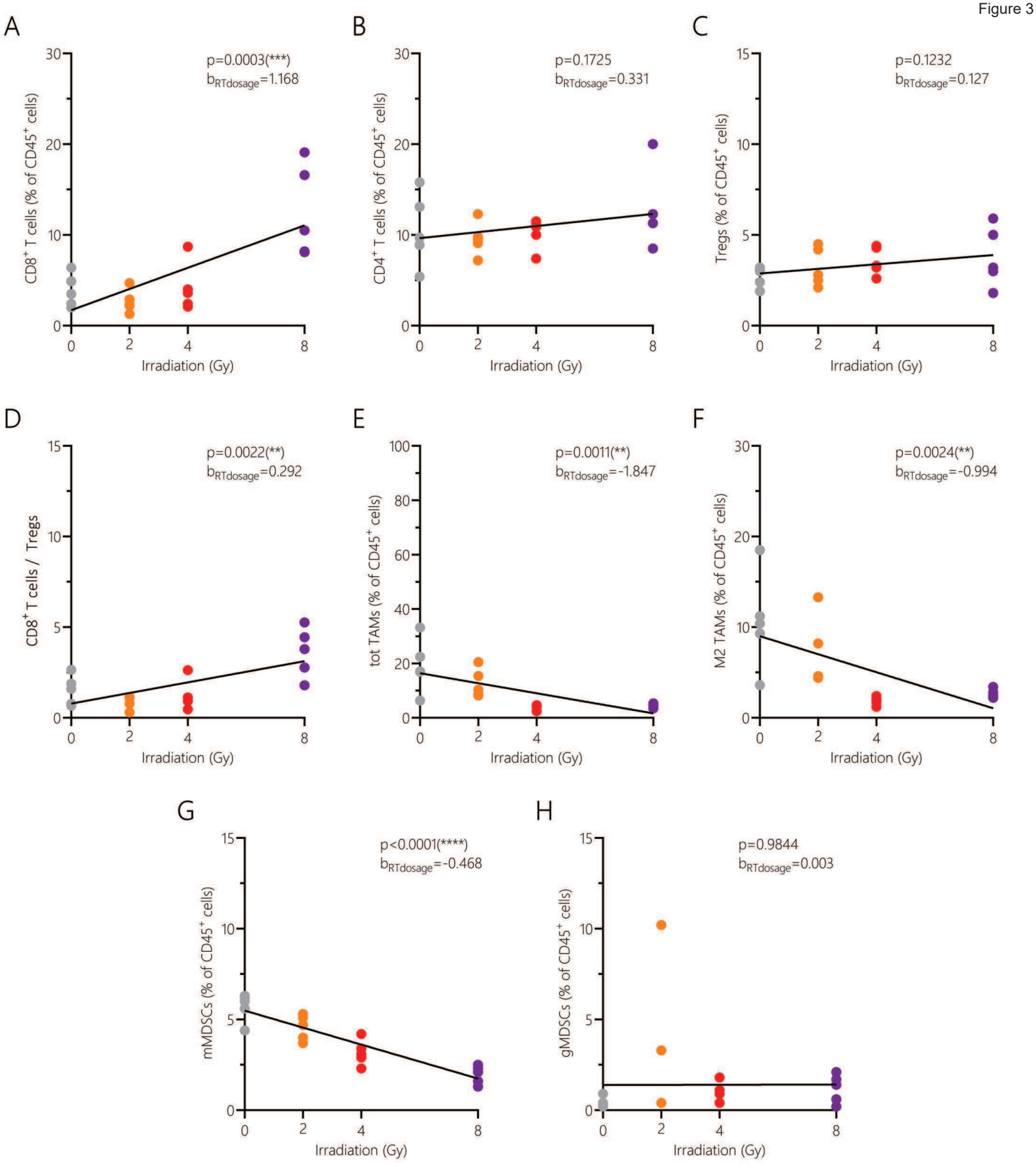
A
p=0.0003(***)
$b_{RTdosage}$=1.168
CD8+ T cells (% of CD45+ cells)
Irradiation (Gy)
B
p=0.1725
$b_{RTdosage}$=0.331
CD4+ T cells (% of CD45+ cells)
Irradiation (Gy)
C
p=0.1232
$b_{RTdosage}$=0.127
Tregs (% of CD45+ cells)
Irradiation (Gy)
D
p=0.0022(**)
$b_{RTdosage}$=0.292
CD8+ T cells / Tregs
Irradiation (Gy)
E
p=0.0011(**)
$b_{RTdosage}$=-1.847
tot TAMs (% of CD45+ cells)
Irradiation (Gy)
F
p=0.0024(**)
$b_{RTdosage}$=-0.994
M2 TAMs (% of CD45+ cells)
Irradiation (Gy)
G
p<0.0001(****)
$b_{RTdosage}$=-0.468
mMDSCs (% of CD45+ cells)
Irradiation (Gy)
H
p=0.9844
$b_{RTdosage}$=0.003
gMDSCs (% of CD45+ cells)
Irradiation (Gy)

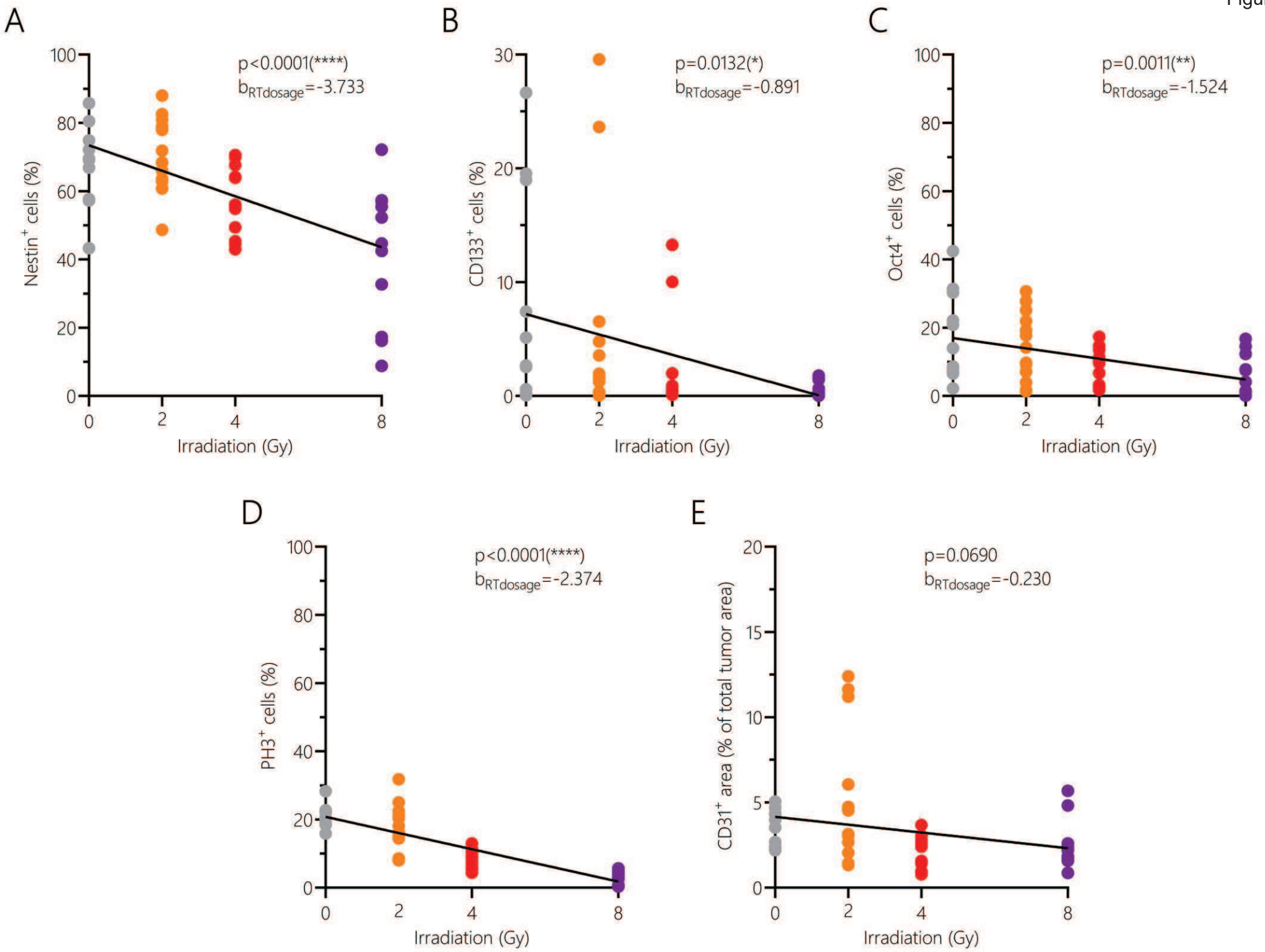
A
p<0.0001(****)
b_RTdosage=-3.733
Nestin+ cells (%)
Irradiation (Gy)
B
p=0.0132(*)
b_RTdosage=-0.891
CD133+ cells (%)
Irradiation (Gy)
C
p=0.0011(**)
b_RTdosage=-1.524
Oct4+ cells (%)
Irradiation (Gy)
D
p<0.0001(****)
b_RTdosage=-2.374
PH3+ cells (%)
Irradiation (Gy)
E
p=0.0690
b_RTdosage=-0.230
CD31+ area (% of total tumor area)
Irradiation (Gy)

Figure 5

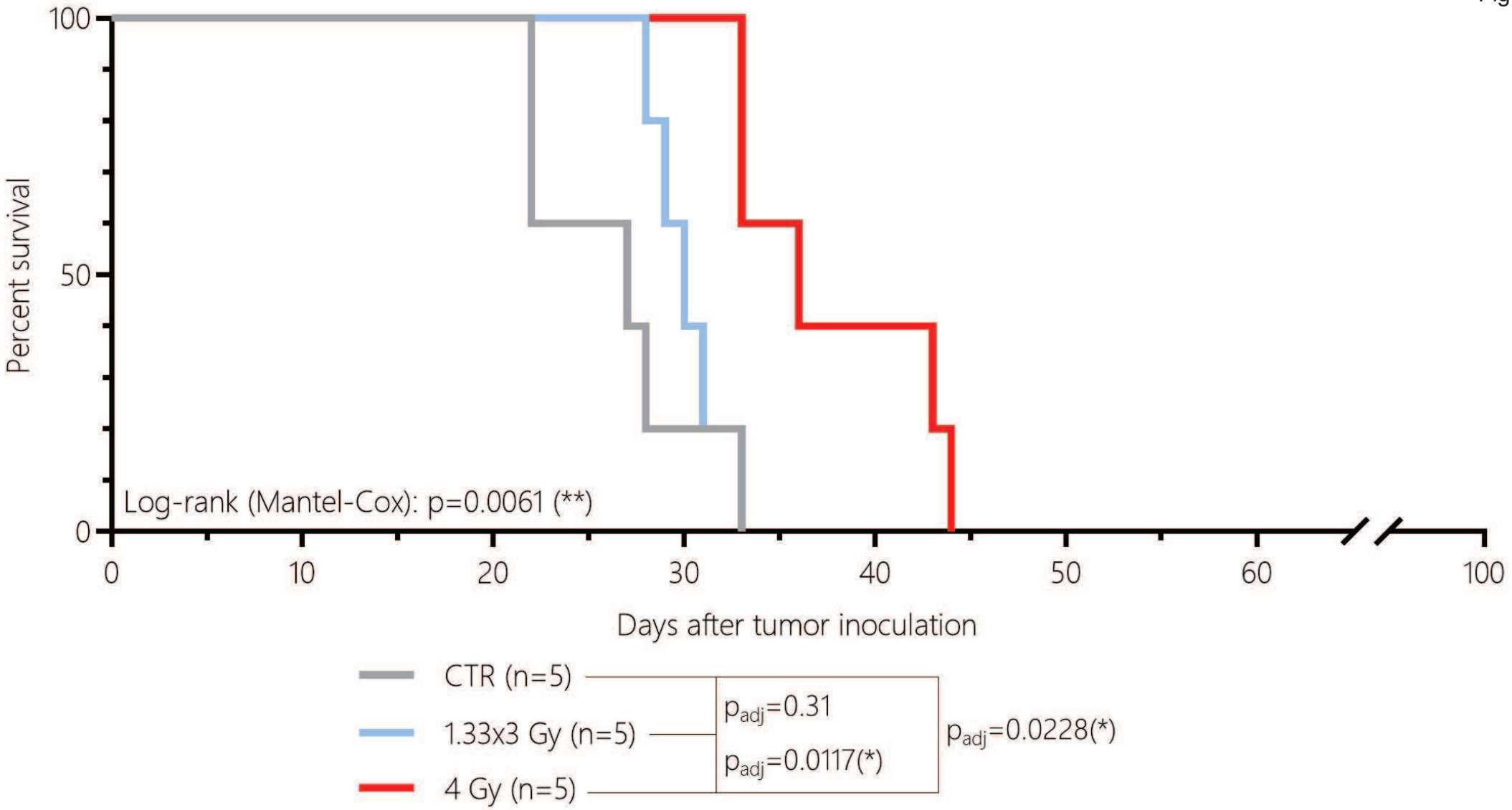

Comparison	Original P value	Benjamini-Hochberg adjusted P value	Benjamini-Hochberg P value threshold	Significant
CTR vs 4 Gy	0.0076	0.0228	0.016	Yes(*)
1.33x3 Gy vs 4 Gy	0.0078	0.0117	0.033	Yes(*)
CTR vs 1.3x3 Gy	0.31	0.31	0.05	No

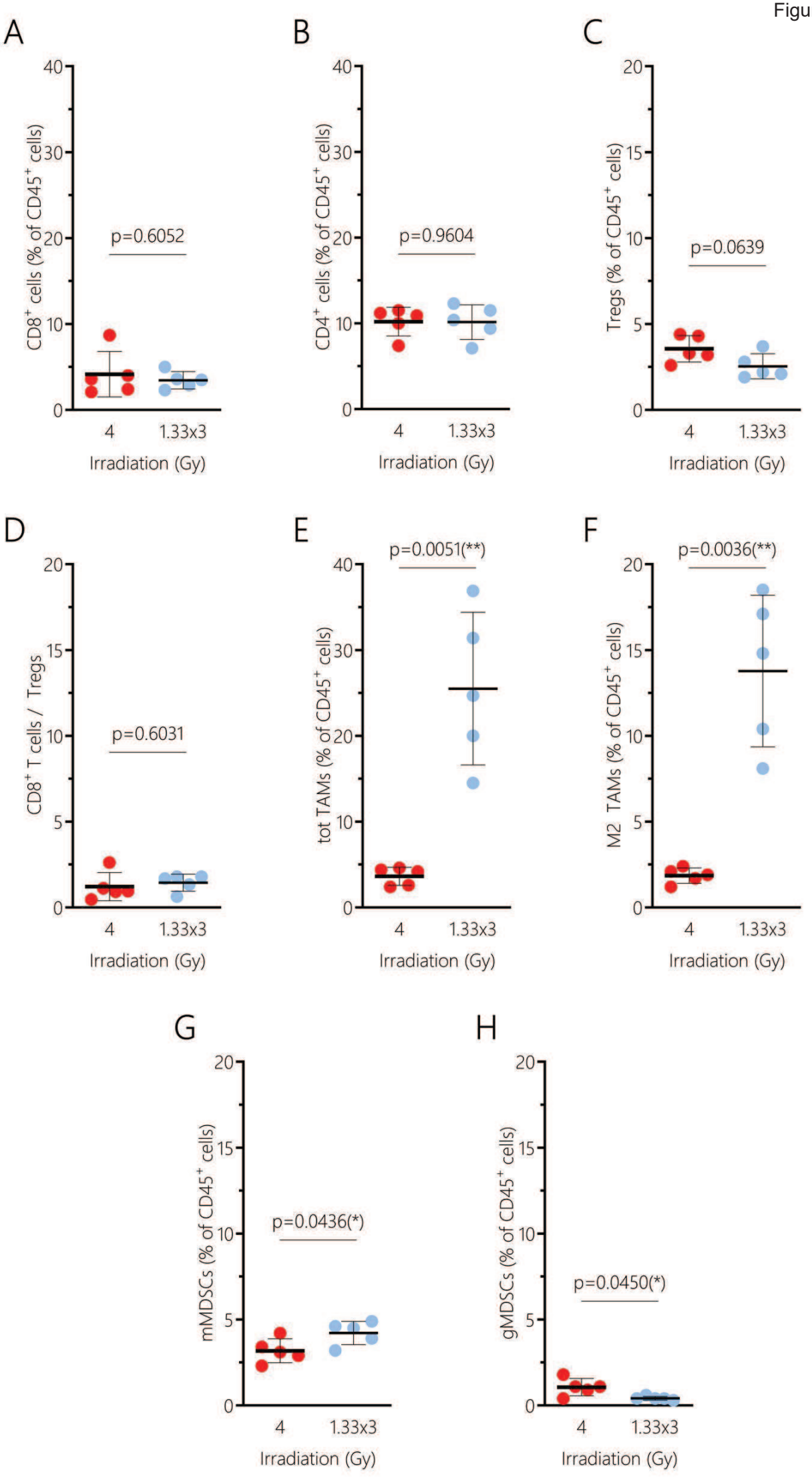
A
CD8+ cells (% of CD45+ cells)
p=0.6052
B
CD4+ cells (% of CD45+ cells)
p=0.9604
C
Tregs (% of CD45+ cells)
p=0.0639
D
CD8+ T cells / Tregs
p=0.6031
E
tot TAMs (% of CD45+ cells)
p=0.0051(**)
F
M2 TAMs (% of CD45+ cells)
p=0.0036(**)
G
mMDSCs (% of CD45+ cells)
p=0.0436(*)
H
gMDSCs (% of CD45+ cells)
p=0.0450(*)
4
1.33x3
Irradiation (Gy)

Figure 7

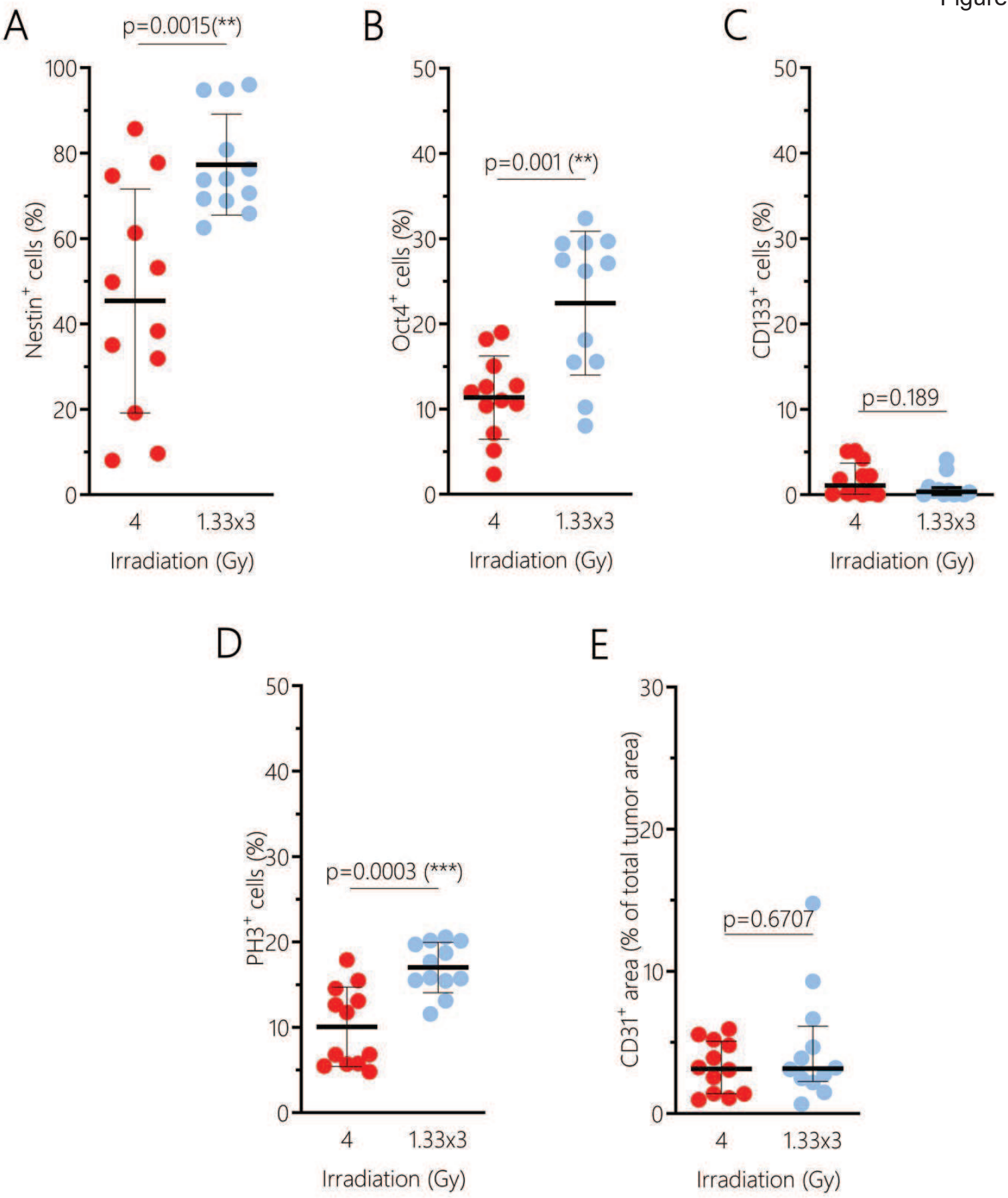
A
p=0.0015(**)
Nestin+ cells (%)
100
80
60
40
20
0
4
1.33x3
Irradiation (Gy)
B
p=0.001 (**)
Oct4+ cells (%)
50
40
30
20
10
0
4
1.33x3
Irradiation (Gy)
C
p=0.189
CD133+ cells (%)
50
40
30
20
10
0
4
1.33x3
Irradiation (Gy)
D
p=0.0003 (***)
PH3+ cells (%)
50
40
30
20
10
0
4
1.33x3
Irradiation (Gy)
E
p=0.6707
CD31+ area (% of total tumor area)
30
20
10
0
4
1.33x3
Irradiation (Gy)

Supplementary material

1) Supplementary figures

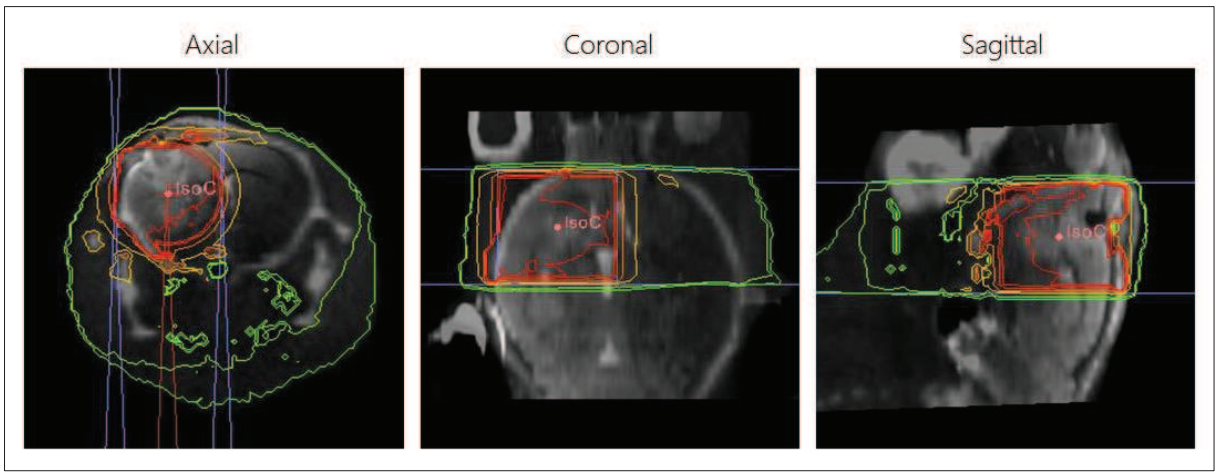

Figure S1. Example of RT treatment plan. On merged MRI-CBCT images, the irradiation isocenter (IsoC) was placed visually at the center of the tumor. By using a 5mm collimator, all the tumor tissue received the prescribed dose whereas most of the surrounding brain tissue was spared.

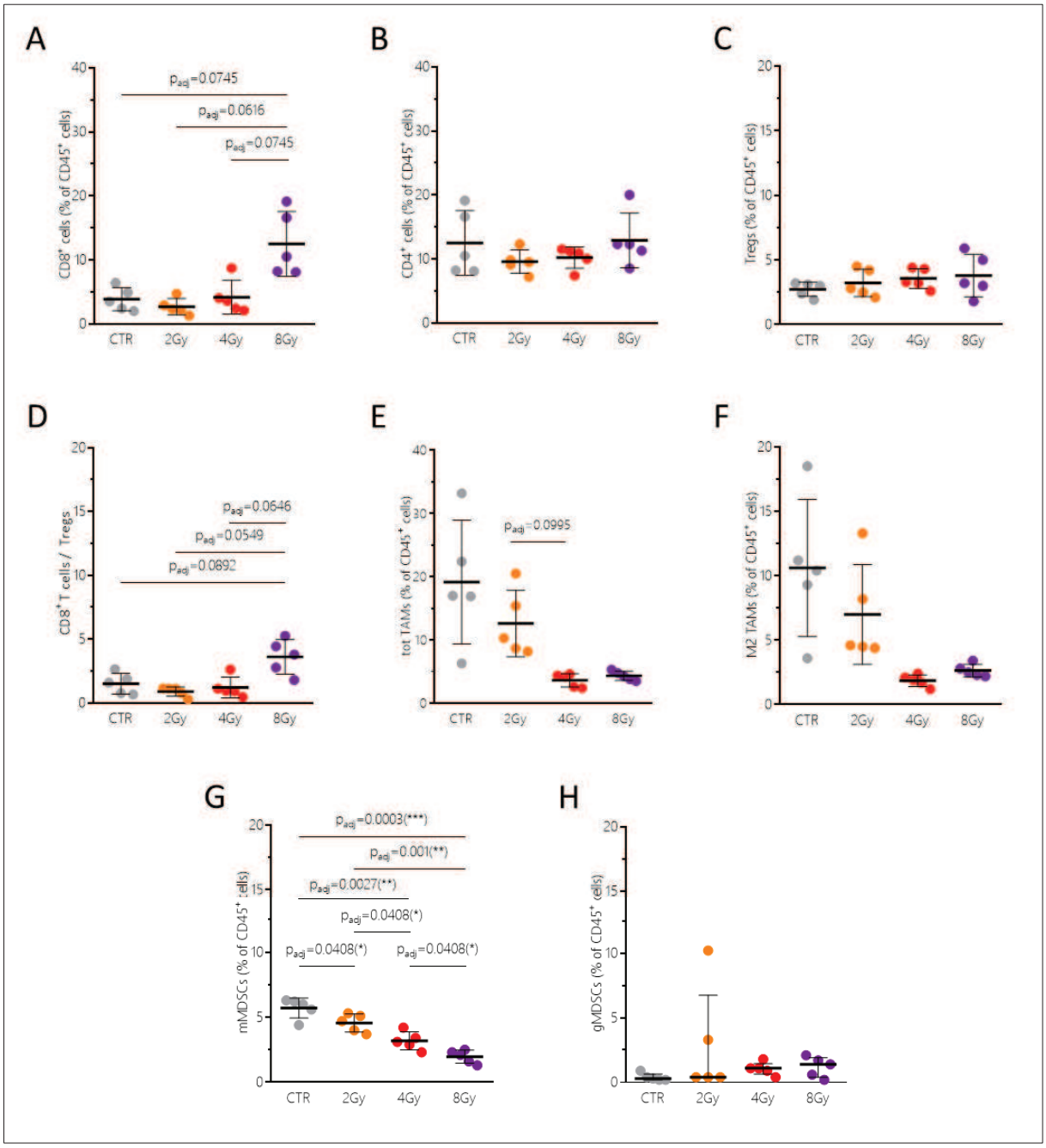

Figure S2. Supplementary analysis of the modifications of the tumor-immune microenvironment induced by RT dose-escalation. NS/CT-2A HGG-bearing mice were treated with 2, 4 or 8 Gy given in one single administration while control mice were left untreated. Tumor-infiltrating immune cells were analyzed with flow-cytometry 7 days after the treatment. The RT dosages were considered as discrete variable and data were compared using ANOVA. Abbreviations. RT: radiotherapy; HGG: high-grade gliomas; CTR: control mice; CD: cluster of differentiation; Tregs: regulatory T cells; TAMs: tumor associated macrophages/microglia; m and gMDSCs: monocytic and granulocytic myeloid-derived suppressor cells

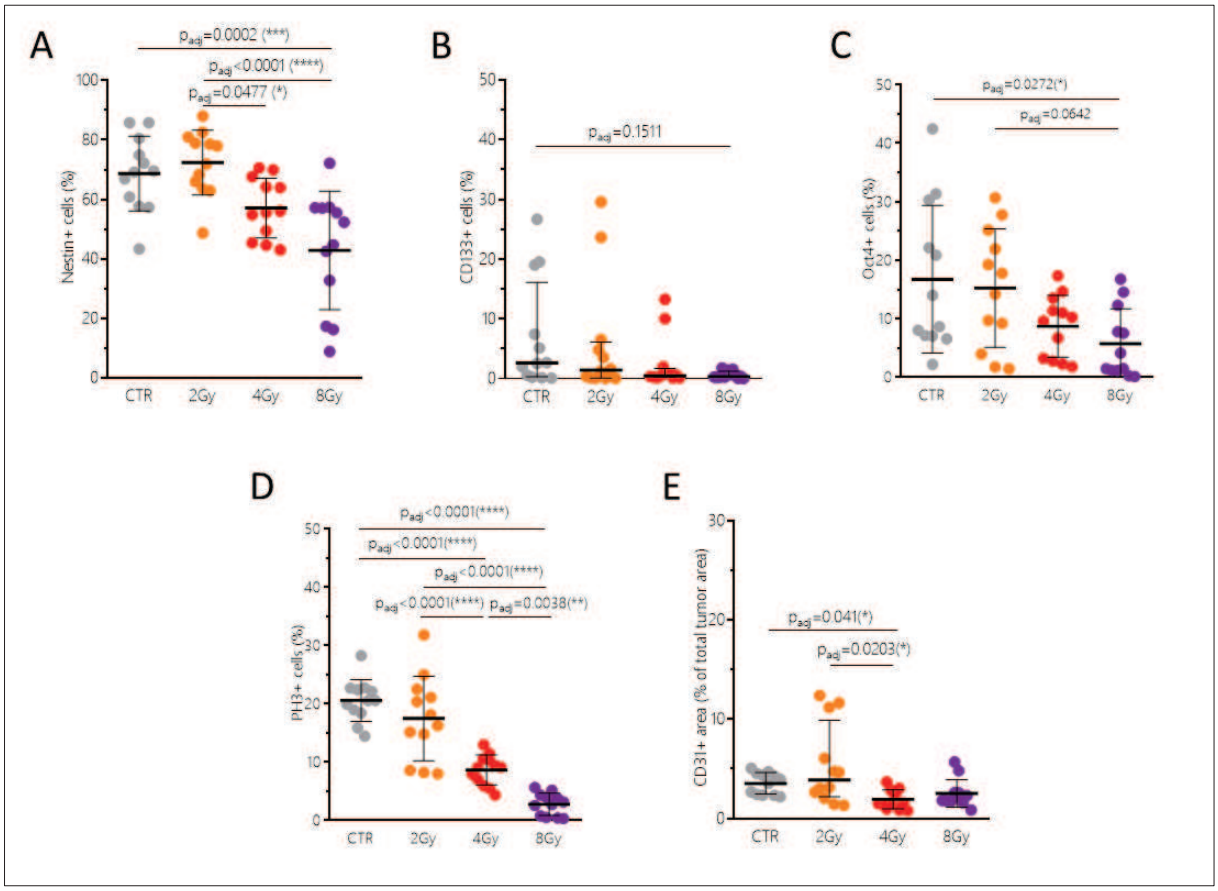

Figure S3. Supplementary analysis of the impact of RT dose-escalation on GSCs, tumor vasculature and tumor cell replication. NS/CT-2A HGG-bearing mice were treated with 2, 4 or 8 Gy given in one single administration while control mice were left untreated. Seven days after treatment, brains were collected and stained for IHC. The RT dosages were considered as discrete variable and data were compared using ANOVA. Abbreviations. RT: radiotherapy; HGG: high-grade gliomas; CTR: control mice; CD: cluster of differentiation; Oct4: octamer-binding transcription factor 4; PH3: Phosphohistone H3.

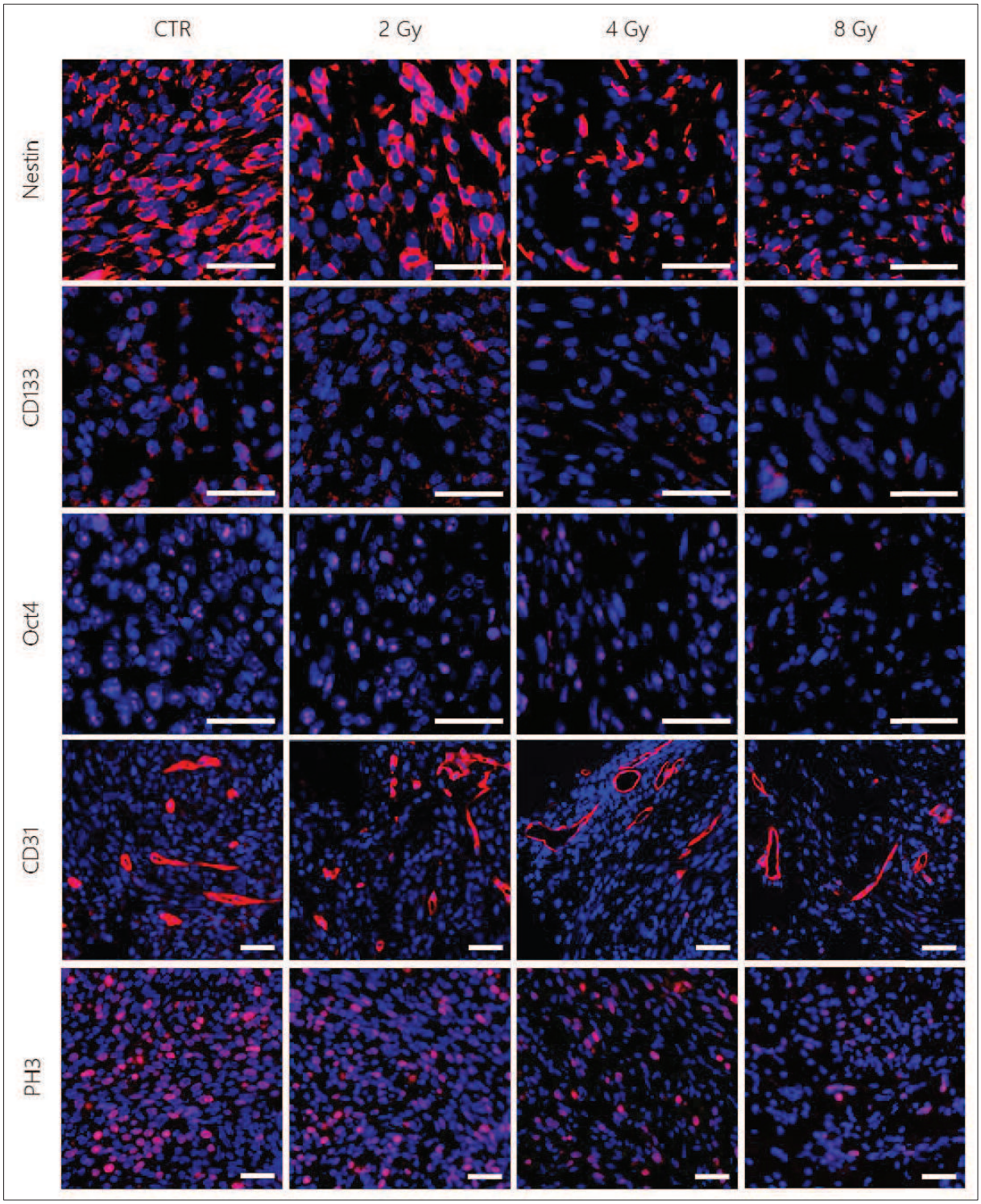

Figure S4. Representative IHC micrograph of Nestin, CD133, Oct4, CD31 and PH3 in the dose-escalation study. Scale bars: 50 µm. Abbreviations. IHC: immunohistochemistry; CD: cluster of differentiation; Oct4: octamer-binding transcription factor 4; PH3: Phosphohistone H3.

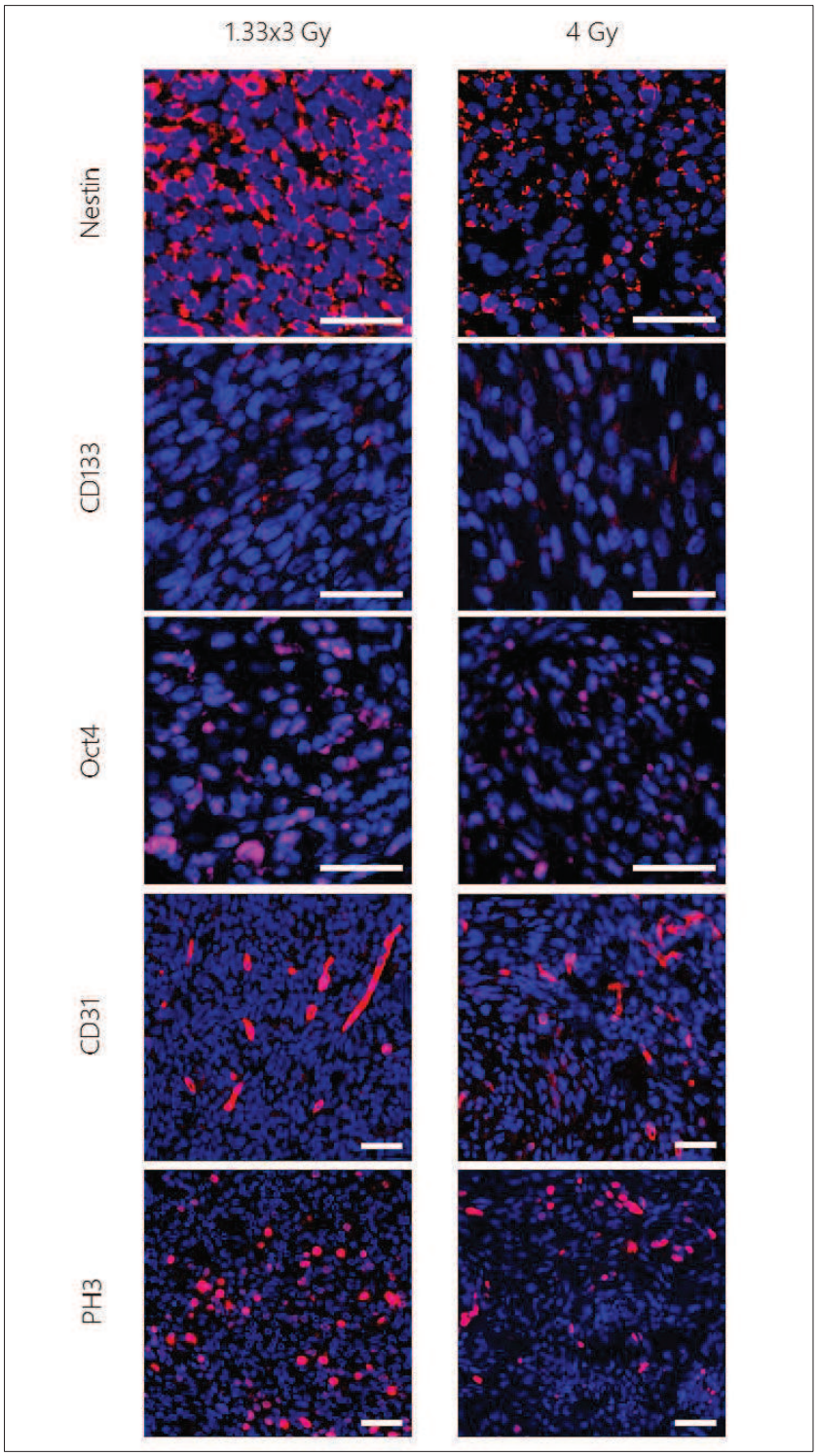

Figure S5. Representative IHC micrograph of Nestin, CD133, Oct4, CD31 and PH3 in the dose-escalation study. Scale bars: 50 µm. Abbreviations. IHC: immunohistochemistry; CD: cluster of differentiation; Oct4: octamer-binding transcription factor 4; PH3: Phosphohistone H3.

2) Supplementary tables

T cells			
Target	**Fluorophore**	**Clone**	**Company**
FVD	eFluor 780	-	Thermofisher
CD45	APC	104	eBioscience
CD3	APC eFluor780	145-2C11	eBioscience
CD4	PerCP Cy5.5	RM4-5	eBioscience
CD8	BV421	53-6.7	BD Biosciences
FoxP3	AF488	R16715	BD Biosciences
Tumor associated mactophages/microglia			
Target	**Fluorophore**	**Clone**	**Company**
FVD	eFluor 780	-	Thermofisher
CD11b	PerCp Cy5.5	M1/70	eBioscience
CD45	APC	104	eBioscience
Ly6G	Fitc	1A8	BD Biosciences
F4/80	BV421	T45-2342	BD Biosciences
CD206	PE	C068C2	Biolegend
Myeloid-derived suppressor cells			
Target	**Fluorophore**	**Clone**	**Company**
FVD	eFluor 780	-	Thermofisher
CD11b	PerCp Cy5.5	M1/70	eBioscience
Ly6G	Fitc	1A8	BD Biosciences
Ly6C	APC eFluor780	HK1.4	Invitrogen

Table S1. Flow-cytometry antibodies.